Measurements of Flow Mixing at Subchannels in a Wire-Wrapped 37-Rod Bundle for a Sodium Cooled Fast Reactor

Hyungmo Kim*, Hwang Bae, Seok-Kyu Chang, Sun Rock Choi, Dong Won Lee, Yung Joo Ko, Hae Seob Choi, Dong-Jin Euh, and Hyeong-Yeon Lee
Korea Atomic Energy Research Institute, 989-111 Daedeok-daero, Yuseong-gu, Daejeon, 305-353, Korea
**Corresponding author: hyungmo@kaeri.re.kr*

1. Introduction

For a safety analysis in a core thermal design of a sodium-cooled fast reactor (SFR), flow mixing characteristics at subchannels in a wire-wrapped rod bundle are very important. Wrapped wires make a cross flow in a around the fuel rod) of the fuel rod, and this effect lets flow be mixed [1, 2]. Experimental results of flow mixing can be meaningful for verification and validation of thermal mixing correlation in a reactor core thermo-hydraulic design code.

A wire mesh sensing technique can be useful method for measuring of flow mixing characteristics. A wire mesh sensor has been traditionally used to measure the void fraction of a two-phase flow field, i.e. gas and liquid [3]. However, it has been recently reported that the wire mesh sensor can be used successfully to recognize the flow field in liquid phase by injecting a tracing liquid with a different level of electric conductivity [4]. This can be powerfully adapted to recognize flow mixing characteristics by wrapped wires in SFR core thermal design. In this work, we conducted the flow mixing experiments using a custom designed wire mesh sensor.

2. Experimental methods

2.1 Test loop

All experiments were conducted at the FIFFA' (Flow Identification test loop for Fast reactor Fuel Assembly) test facility at KAERI. The test loop consists of a tracing water tank, fuel rod with inside tube for water injection, and wire mesh sensor at the end of test rig. Fig. 1 shows a schematic drawing of our test loop.

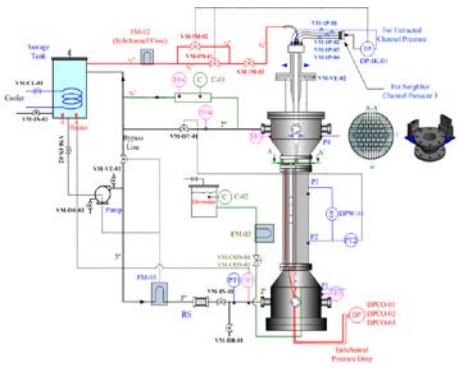

Fig. 1. Schematic drawing of the test loop (FIFFA).

2.2 Design of a wire mesh sensor

A wire mesh system consists of a sensor and an electronic part. The sensor has both a transmitting electrode layer and receiving electrode layer with a short distance and an angle of 90°. As a driving voltage is supplied to the transmitting electrode layer, a current is derived in the receiving electrode layer. According to the electric conductivity level of the liquid between two layers, the derived currents are varied. Using this principle, a difference in the electric conductivity of the liquid across the cross points can be measured.

Our wire mesh sensor was installed 5mm above the upper end of wire-wrapped 37-pin fuel assembly. A cross point of the wires is fabricated to be located at the center or beside each subchannel. Active transmitting and receiving electrode wires consist of 16 × 16 channels, respectively. The schematic drawing and assembled pictures of the wire mesh sensor are shown in Fig. 2.

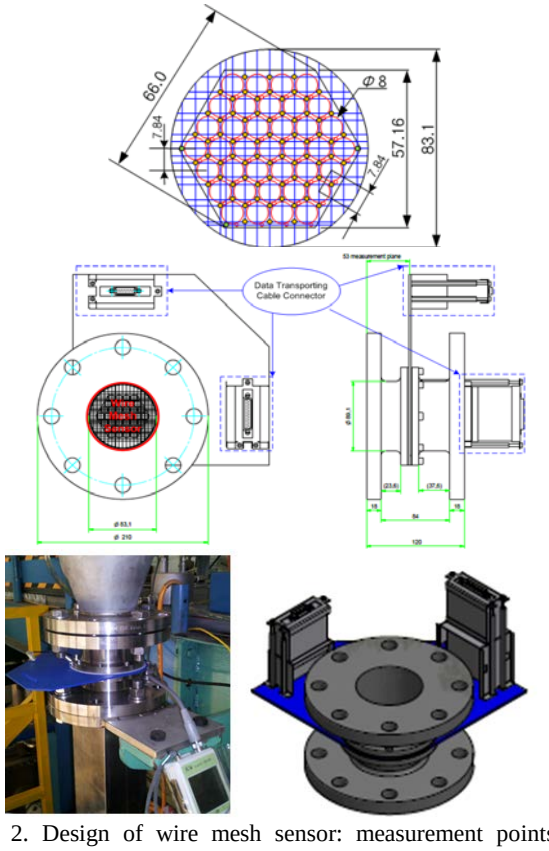

Fig. 2. Design of wire mesh sensor: measurement points, schematics, and an assembled image.

2.3 Experimental conditions

Geometry parameters are designed with a pitch to diameter ration (*P/D)* of 1.14 and wire lead length to diameter ratio (*H/D)* of 27.7. Hydrodynamic similarity with a SFR core is considered by matching these two geometric conditions (i.e., P/D and H/D) and Reynolds number (*Re* = 37,110).

A wire mesh sensor can receive electric conductivity level as integer values from 0 to 4079 (12 bits). We used deionized (DI) water as a background liquid, and tap water was injected as a tracing liquid. Because the conductivity of tap water is much higher than DI water, it is useful tracing liquid. The sensor gain was fixed as 100, and sampling frequency was also selected as 100 Hz. Every measurement was continued for 20 s ⇒ Measurements were conducted continuously with every 20 seconds including both homogeneous (~5 s) and injecting stage (~5 s) as shown in Fig. 3.

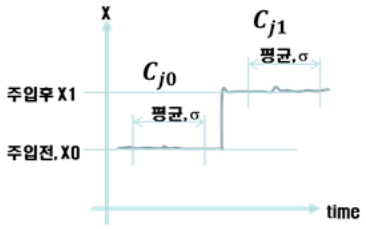

Fig. 3. Data acquisition procedure of each test.

3. Results and discussion

3.1 Post-processing method

$$C_{j,n} = \frac{C_{j1} - C_{j0}}{\sum_j A_j \ (C_{j1} - C_{j0})/(\sum_j A_j)} \qquad (1)$$

Eq. (1) shows present post-processing method considered both the unit cell area and the local value differences in homogeneous liquid. Especially, because our wire mesh sensor was designed as an irregular type, weighting value was essentially represented in Eq. (1). From this process, we had two major benefits. First, uniformity in a homogeneous state is extremely increased as shown in Fig. 4. Second, we can normalize the data in spite of conductivity increase of a background liquid as repeating experiments.

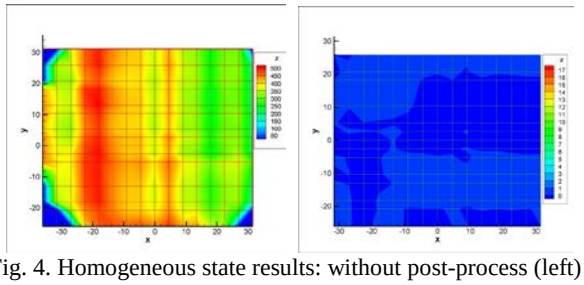

Fig. 4. Homogeneous state results: without post-process (left) and after post-processing result (right) in a homogeneous state.

3.2 Flow mixing results

Fig. 5 represents the flow fields from the flow mixing experiments using the wire mesh sensor and the post-processing method. In the case of an inner subchannel injection, injected liquid gradually diffused as shown in upper results (1L and 1S) of Fig. 5, because the cross flow by wrapped wires is almost eliminated for the opposite direction cross flow collision. However, in the case of an edge subchannel, all cross flow by wrapped wires should have the same direction: a clockwise direction without collisions. So, the peak point of the flow field should move around as edge walls of the fuel assembly as shown in lower results (25L and 25S) of Fig. 5.

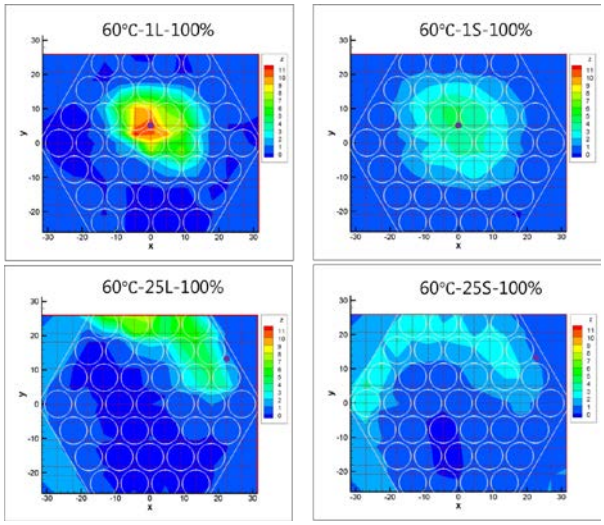

Fig. 5. Flow mixing results (*Re* = 37,110).

3.3 Uncertainty analysis

The uncertainty analysis was also conducted. The temperature (T), and flow rate (M) variations were considered as the system error components in experiments. The methodology of system error calculations is shown in Eq. (2).

$$(\delta C_{j,n})^2 = \left(\frac{\partial C_{j,n}}{\partial C_{j1}}\right)^2 (\delta C_{j1})^2 + \left(\frac{\partial C_{j,n}}{\partial C_{j0}}\right)^2 (\delta C_{j0})^2$$

$$\left(\frac{\partial C_{j,n}}{\partial B}\right)^2 (\delta B)^2 = \left(\frac{\partial C_{j,n}}{\partial C_{j1}}\right)^2 \left(\frac{\partial C_{j1}}{\partial B}\right)^2 (\delta B)^2 + \left(\frac{\partial C_{j,n}}{\partial C_{j0}}\right)^2 \left(\frac{\partial C_{j0}}{\partial B}\right)^2 (\delta B)^2$$

$$= \left(\frac{\left(\sum_j A_j - C_{j,n} A_j\right)}{\sum_j \{A_j (C_{j1} - C_{j0})\}}\right)^2 \left\{\left(\frac{\partial C_{j1}}{\partial B}\right)^2 + \left(\frac{\partial C_{j0}}{\partial B}\right)^2\right\} (\delta B)^2$$

$$\left(\frac{\partial C_{j,n}}{\partial B}\right)(\delta B) = \frac{\left(\sum_j A_j - C_{j,n} A_j\right)}{\sum_j \{A_j (C_{j1} - C_{j0})\}} \sqrt{\left(\frac{\partial C_{j1}}{\partial B}\right)^2 + \left(\frac{\partial C_{j0}}{\partial B}\right)^2} (\delta B) \ : \text{B기인오차} \qquad (2)$$

The random error was obtained from Eq. (3).

$$\delta C_{j,n} = \frac{\left(\sum_j A_j - C_{j,n} A_j\right)}{\sum_j \{A_j (C_{j1} - C_{j0})\}} \sqrt{(\delta C_{j1})^2 + (\delta C_{j0})^2} \qquad (3)$$

Table I shows the estimated results of the system errors (from T, and M) and the random error. Though the order of magnitude of the peak values is about 10, the estimated errors were very small values.

Table I: The estimated errors: system and random error

	error from δT (95%)	error from δM (95%)	random error (95%)
1L	1.827e-3	1.146e-6	0.087
1S	1.405e-3	1.119e-6	0.042
25L	5.59e-4	1.373e-6	0.072
25S	6.69e-4	7.64e-7	0.045

4. Conclusions

To verify and validate computer codes for the SFR core thermal design, mixing experiments were conducted at a hexagonally arrayed 37-pin wire-wrapped fuel rod bundle test section. The well-designed wire mesh sensor was used to measure flow mixing characteristics. The developed post-processing method has its own merits, and flow mixing results were reasonable. In addition, by uncertainty analysis, the system errors and the random error were estimated in experiments. Therefore, the present results and methods can be used for design code verification and validation.

ACKNOWLEDGMENTS

This work was supported by the National Research Foundation of Korea (NRF) grant funded by the Korea government (MEST) (No. 2013K1A3A7A03078195).

REFERENCES

[1] S.-K. Cheng and N. E. Todreas, Hydrodynamic Models and Correlations for Bare and Wire-Wrapped Hexagonal Rod Bundles – Bundle Friction Factors, Subchannel Friction Factors and Mixing Parameters, Nuclear Engineering and Design, Vol.92, p. 227, 1986.

[2] J.J. Lorenz and T. Ginsberg, Coolant Mixing and Subchannel Velocities in an LMFBR Fuel Assembly, Nuclear Engineering and Design, Vol.40, p.315, 1977.

[3] A. Ylönen, W.-M. Bissels, and H.-M. Prasser, Single-Phase Cross-Mixing Measurements in a 4X4 Rod Bundle, Nuclear Engineering and Design, Vol.241, p.2484, 2011.

[4] H.-M. Prasser, A. Böttger, and J. Zschau, A New Electrode-Mesh Tomograph for Gas-Liquid Flows, Flow Measurement and Instrument, Vol.9, p. 111, 1998.